1040-5488/97/7411-0926$03.00/0 VOL. 74, NO. 11, PP. 926–930
OPTOMETRY AND VISION SCIENCE


ORIGINAL ARTICLE

# Mathematical Model of a Placido Disk Keratometer and Its Implications for Recovery of Corneal Topography

**RICHARD H. RAND, ScD, HOWARD C. HOWLAND, PhD, and RAYMOND A. APPLEGATE, OD, PhD, FAAO**

*Department of Theoretical and Applied Mechanics (RHR) and Section of Neurobiology and Behavior (HCH), Cornell University, Ithaca, New York and Department of Ophthalmology, University of Texas Health Science Center at San Antonio, San Antonio, Texas (RAA)*

**ABSTRACT: The purpose of this paper is to illustrate the importance of radial contours in the target pattern of a Placido disk keratometer. We do so by presenting an example of a corneal surface which cannot be determined solely by the use of Placido ring images, but rather which requires radial contours for its determination. In order to prove our assertions, we derive partial differential equations (called the corneal transform), which relate the ring targets to their images. (Optom Vis Sci 1997;74:926–930)**

Key Words: videokeratometer, keratometry, cornea, Placido disk

The advent of refractive corneal surgery on a large scale has stimulated interest in the precise shape of the cornea and has led to the proliferation of machines to measure the cornea's topography. A majority of these machines work on the principle of deducing corneal shape by capturing the image of a target reflected from the surface of the cornea. The image is usually recorded by a video camera and stored in the memory of a digital computer for later processing. All of the machines use some device for accurately positioning the apex of the cornea relative to the optic axis of the machine. Modern methods of measuring corneal topography have been reviewed by Applegate and Howland.[1]

Most corneal topographers have retained the traditional Placido disk ring target, although at least one has not.[2] Given the near spherical shape of the cornea, it seems only reasonable that the target has circular symmetry. Curiously, however, none of the early machines included radial lines or any other radial features which would allow the precise identification of points on the image with points on the target. Indeed, the general assumption of all such machines has been that points on the image and points on the target lie in a plane which contains the optic axis of the machine. Of course, this need not be so, and it has been suspected that this assumption could lead to errors in the reconstruction of a corneal surface.[1, 3]

Recently, Klein[4] asserted, and we agree with him, that, in principle, any sufficiently smooth corneal surface which could be represented accurately by a polynomial expansion could also be reconstructed from Placido disk images. (Whether a particular machine in fact does this accurately is another question.) However, there is an infinitude of surfaces which contain discontinuities and hence cannot be so reconstructed. Klein's method is based on iterative ray tracing whereby, starting from a known target pattern and a known reflected image of the cornea, the assumed corneal shape is altered until the pattern it reflects matches the pattern actually obtained. If the actual corneal surface is everywhere continuous and can be represented by a polynomial, Klein has found in modeling experiments that his methods always converge on a solution.[5]

We wished to examine this question more carefully and, hence, were led to find an analytical relationship between the image pattern and the target pattern for a given corneal shape. These relationships are presented in this paper, and it will be seen from our results that there are indeed important corneal shapes which cannot be recovered by Placido disk keratometers which use targets consisting solely of rings.

## CORNEAL TRANSFORM

Our goal in this section is to present equations which relate a given image to its corresponding target pattern. The cornea is represented by a surface which is described by a function $z = f(x, y)$. A target pattern on a source plane $z = z_s$ is reflected off of the cornea and collected by a telecentric lens system, which is assumed to eliminate all reflected rays except those in the z direc-

tion, i.e., perpendicular to the source plane (see Figs 1 and 2). In Appendix I we derive the following relation between the location $(x_s, y_s)$ of a generic point P on the source plane, and the location (x, y) on the cornea of the reflected image Q of source point P.

$$x_s = x + \frac{2(z_s - f)}{f_x^2 + f_y^2 - 1} f_x, \quad y_s = y + \frac{2(z_s - f)}{f_x^2 + f_y^2 - 1} f_y \qquad (1)$$

where $f_x$ and $f_y$ represent partial derivatives of the corneal surface function f(x, y). For a given corneal shape f(x, y), equation 1 gives the location of a source point $P(x_s, y_s)$ (in the target plane) in terms of the location of a reflected point Q(x, y) (in the image plane). Equation 1 is referred to as the corneal transform.

Because the cornea is nearly spherical, and because the usual target pattern consists of concentric circles, it is mathematically convenient to work in polar coordinates:

$$x = r \cos \theta, \quad y = r \sin \theta \qquad (2)$$

$$x_s = r_s \cos \theta_s, \quad y_s = r_s \sin \theta_s. \qquad (3)$$

Here $(r, \theta)$ represents the polar coordinates of a point in the image plane, whereas $(r_s, \theta_s)$ represents the polar coordinates of a point in the target plane.

In Appendix II we derive the following polar coordinate version of equation 1:

$$r_s^2 = r^2 + 2Hrf_r + H^2\left(f_r^2 + \frac{f_\theta^2}{r^2}\right) \qquad (4)$$

$$\theta_s = \theta + \arctan\left(\frac{Hf_\theta}{r^2 + Hrf_r}\right) \qquad (5)$$

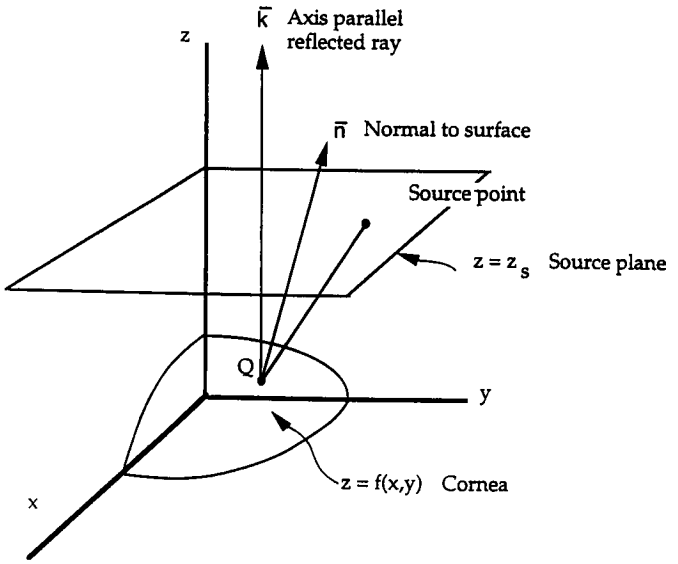


**FIGURE 1.**

Geometry of the Placido disk keratometer model. A ray from a source point on the source plane is reflected off of the surface of the cornea represented by the function f(x, y) to form an axis parallel ray, $\bar{k}$. The telecentric stop shown in Fig. 2 guarantees that only axis parallel rays form the image of the target.

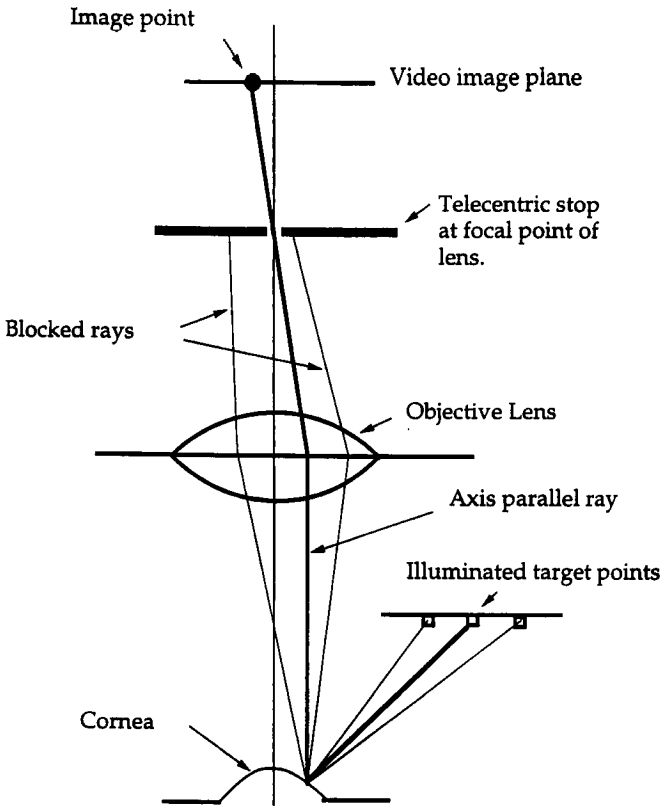


**FIGURE 2.**

Optics of the envisioned Placido disk keratometer. Illuminated target points at the source plane are reflected from the cornea. However, the telecentric stop guarantees that only axis parallel rays are imaged at the video image plane.

where $f_r$ and $f_\theta$ represent partial derivatives of the corneal surface function $f(r, \theta)$, now considered as a function of r and $\theta$, and where the quantity H is given by:

$$H = \frac{2(z_s - f)}{f_r^2 + (1/r^2)f_\theta^2 - 1}. \qquad (6)$$

Note that for an arbitrary point $(r, \theta)$ on a given image $f(r, \theta)$, equations 4 and 5 give the location of a point $(r_s, \theta_s)$ on the target plane.

## EXAMPLE

Because the cornea is nearly spherical, it is convenient to represent z = f(x, y) as the sum of a perfect sphere of radius R and a deviation from a sphere. We write f(x, y) in the form:

$$f(x, y) = \sqrt{R^2 - x^2 - y^2} + g(x, y) \qquad (7)$$

or, in polar coordinates,

$$f(r, \theta) = \sqrt{R^2 - r^2} + g(r, \theta) \qquad (8)$$

where R is the radius of a reference sphere and where g(x, y) is a function representing the deviation of the cornea from a perfect spherical surface.

To illustrate the need for radial contours, we take the case where $g(r, \theta)$ is of the form:

$$g(r, \theta) = \begin{cases} \epsilon \sin 8\theta & \text{for } r \geq 2 \text{ mm} \\ 2(r - 1.5)\epsilon \sin 8\theta & \text{for } 1.5 < r < 2 \text{ mm} \\ 0 & \text{for } r \leq 1.5 \text{ mm} \end{cases} \quad (9)$$

where $\epsilon$ is a parameter representing the magnitude of g (see Fig. 3). This function g could provide a simplified model for a cornea that has been surgically modified by an eight-cut radial keratotomy. The region inside a circle of radius 2 mm is taken to be spherical. The region outside of radius 2.1 mm consists of a spherical surface plus a small amplitude sinusoidal shape which involves eight symmetrically placed peaks. The small region between these two regions is a transition zone used to avoid a spatial discontinuity.

We wish to examine the relationship between the corneal shape (equations 8 and 9) and the image it produces on a keratometer. However, because the corneal transform equations (equations 4 and 5) give the target location as a function of the image location, we shall instead examine the shape of a target that would produce an image consisting of circles and radial lines. Because the corneal shape is very nearly spherical, this procedure will provide us with a similar pattern to that which would be produced on a keratometer image due to a target of circles and radial lines.

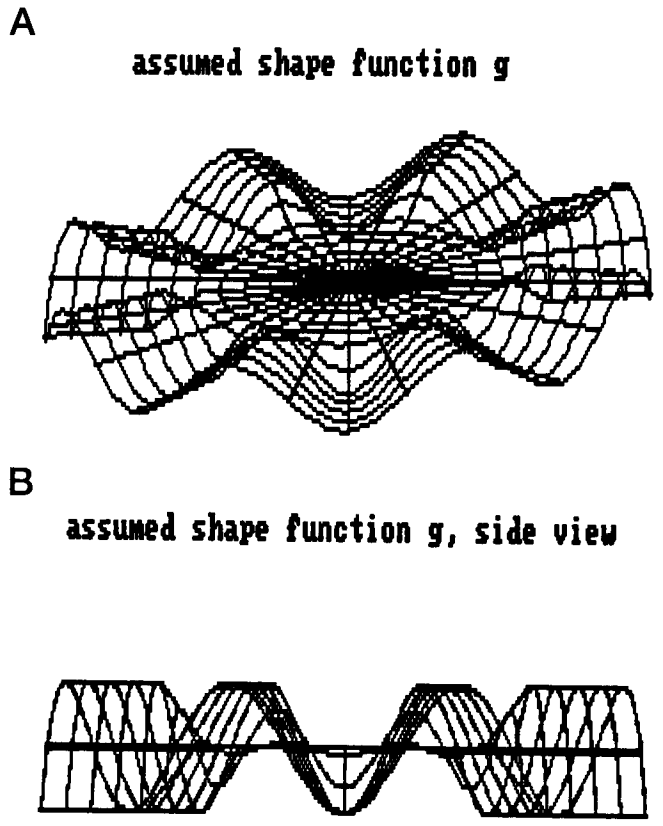


**FIGURE 3.**

Shape function, g, used in example, which illustrates that circular mires by themselves are insufficient for the recovery of corneal shape (see Fig. 4 for resulting corneal images). A: Perspective view of shape function. B: Side view of shape function.

In order to obtain numerical results, we take the sample values:

$$\epsilon = 0.01 \text{ mm (magnitude of deviation from sphere, g)} \quad (10)$$

$$R = 7.5 \text{ mm (corneal radius)} \quad (11)$$

$$z_s = 100 \text{ mm (distance from source plane to cornea).} \quad (12)$$

Substituting equations 9 and 8 into the corneal transform (equations 4 and 5) and assuming an image pattern that consists of circles and radial lines, we obtained the corresponding target pattern shown in Fig. 4.

Although from Fig. 4A it is obvious that the serrations have disturbed the pattern of circular mires in the transition region, in the periphery there is no hint of such a disturbance. Inspection of the spoke pattern, Fig. 4B, shows that in the periphery their pattern is indeed disturbed by the serrations, as indicated by the periodic unevenness in their spacing.

## DISCUSSION

Klein[4] has suggested that target patterns composed solely of circular rings incur little error in the determination of corneal surface shapes, and that the inclusion of radial target lines is unimportant. We sought a counter-example and produced equation 9, in which nearly circular target rings are mapped by the corneal transform into circular images, i.e., displacements in the outer region are nearly tangential. This means that virtually no information can be obtained about this region if radial target lines are omitted. Moreover, this example has physical significance in that it offers a model of a radially keratotomized cornea in which a central smooth zone relatively abruptly changes into a furrowed periphery.

Our approach takes into account tangential displacements as reflected in the images of radial target lines. This allows the possibility of recovering the shape of the corneal surface from the keratotomized data. However, a scheme which omitted the radial elements from the target pattern would see only Fig. 4A, which shows nearly circular target patterns corresponding to circular images in the outer region. Note that a cornea which possessed a purely spherical outer region (in which $g = 0$) would display virtually the same image!

We note, however, that our idealized example of equation 9 contains a transition region between $r = 1.5$ mm and $r = 2$ mm, i.e., a relatively abrupt transition separating the two corneal regions. It is possible that the data from this region could be used to obtain an approximation for the corneal surface shape without the use of radial lines in the target pattern.

If a polynomial representation of the corneal surface was sought for an example like that of equation 9, difficulties would be expected because many terms would need to be included in order to capture the surface topography. If the example were altered so that the width of the transition region was reduced to the limiting case of a discontinuity, then a polynomial representation would fail.[4]

Although it is true that normal corneas can be expected not to have discontinuities in their surfaces, normal corneas are not the interesting corneas in the clinical environment. Instead, it is the pathological corneas which are interesting and which are likely to have significant abrupt changes in their shape. Furthermore, if therapeutic keratectomies or photorefractive keratectomies are to

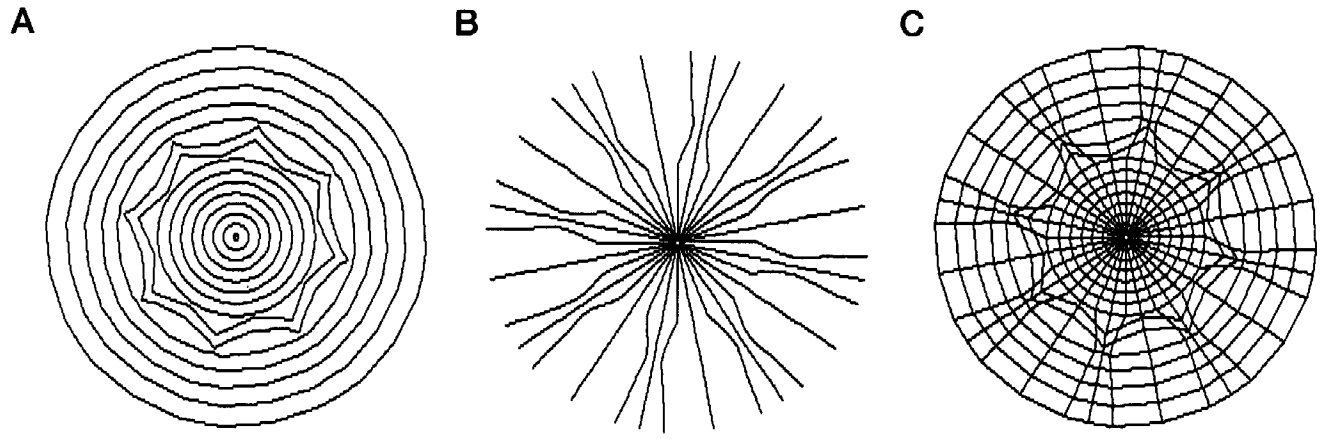


**FIGURE 4.**

Target pattern corresponding to an assumed image of A: circular rings, B: spokes, and C: both circular rings and radial lines, all from a cornea with the shape function, g, of Fig. 3. Note that from the circular mire image of A there is no hint of the peripheral serrations of the cornea outside the transition region.

be guided and/or verified by corneal topography, then accurate measurements of the cornea are of prime importance. For these reasons it would seem prudent to include radial lines in Placido disk keratometer targets and use algorithms that can take advantage of the information they supply.

Finally, we note that although we have assumed that all the target rings lie in the same plane, $z = z_s$, the formulas presented here are applicable to keratometers in which each Placido ring is located at a distinct distance from the cornea, in which case the parameter $z_s$ is permitted to depend on the Placido radius $r_s$.

## APPENDIX I

In this Appendix, we derive equation 1. Referring to Fig. 1, let $\bar{n}$ be the unit normal to the corneal surface at point Q, and suppose the lens system collects only those reflected rays which are in the z direction, $\bar{k}$, i.e., perpendicular to the source plane. Then, optics require that i) $\bar{k}$, $\bar{n}$ and $\overline{QP}$ be coplanar, and ii) the angle of incidence between $\overline{QP}$ and $\bar{n}$ be equal to the angle of reflection between $\bar{k}$ and $\bar{n}$. These requirements may be written:

$$\text{i)}\quad \overline{QP} \cdot (\bar{k} \times \bar{n}) = 0 \tag{13}$$

$$\text{ii)}\quad \frac{\overline{QP}}{|\overline{QP}|} \cdot \bar{n} = \bar{k} \cdot \bar{n}. \tag{14}$$

Let $P:(x_s, y_s, z_s)$ and $Q:(x, y, f(x, y))$. Then $\overline{QP} = (x_s - x, y_s - y, z_s - f(x, y))$. Writing $\bar{k} = (0, 0, 1)$, $\bar{n} = \nabla(z - f(x, y))/|\nabla(z - f(x, y))| = (-f_x, -f_y, 1)/\sqrt{f_x^2 + f_y^2 + 1}$, -condition i) becomes

$$(x_s - x, y_s - y, z_s - f(x, y)) \cdot (0, 0, 1) \times \frac{(-f_x, -f_y, 1)}{\sqrt{f_x^2 + f_y^2 + 1}} = 0 \tag{15}$$

which gives

$$(x_s - x)f_y - (y_s - y)f_x = 0. \tag{16}$$

Condition ii) becomes

$$\frac{(x_s - x, y_s - y, z_s - f(x, y))}{\sqrt{(x_s - x)^2 + (y_s - y)^2 + (z_s - f(x, y))^2}} \cdot (-f_x, -f_y, 1) = (0, 0, 1) \cdot (-f_x, -f_y, 1) \tag{17}$$

or squaring equation 17 and rearranging terms,

$$[f_x(x_s - x) + f_y(y_s - y)]^2 - 2(z_s - f)[f_x(x_s - x) + f_y(y_s - y)] - (x_s - x)^2 - (y_s - y)^2 = 0. \tag{18}$$

Next, solve equation 16 for $x_s - x$:

$$x_s - x = (y_s - y)f_x/f_y \tag{19}$$

and substitute equation 19 into equation 18, which then may be solved for $y_s - y$, giving the second of equation 1. Substituting the result into equation 19 gives the first of equation 1. The second of equation 1 may be similarly obtained.

## APPENDIX II

In this Appendix, we derive the polar form of the corneal transform equations 4 and 5. We begin by writing the rectangular form of the corneal transform, equation 1, in the form:

$$x_s = x + f_x H, \quad y_s = y + f_y H \tag{20}$$

where H is given by equation 6 because

$$f_x = f_r r_x + f_\theta \theta_x = f_r \frac{x}{r} - f_\theta \frac{y}{r^2} \tag{21}$$

$$f_y = f_r r_y + f_\theta \theta_y = f_r \frac{y}{r} + f_\theta \frac{x}{r^2} \tag{22}$$

so that

$$f_x^2 + f_y^2 = f_r^2 + \frac{1}{r^2} f_\theta^2. \tag{23}$$

In order to obtain equation 4, we note that

$$r_s^2 = x_s^2 + y_s^2 \tag{24}$$

and we substiture equation 20, use equation 23, and note that

$$xf_x + yf_y = rf_r. \tag{25}$$

In order to obtain equation 5, we note that

$$\tan \theta_s = \frac{y_s}{x_s} \tag{26}$$

which becomes, using equations 20, 21, and 22,

$$\tan \theta_s = \frac{r \sin \theta + H(f_r \sin \theta + f_\theta(\cos \theta/r))}{r \cos \theta + H(f_r \cos \theta - f_\theta(\sin \theta/r))} \tag{27}$$

which may be written

$$\tan \theta_s = \frac{r \tan \theta + H(f_r \tan \theta + (f_\theta/r))}{r + H(f_r - \tan \theta(f_\theta/r))}. \tag{28}$$

Equation 28 may be simplified by using the identity:

$$\tan(u + v) = \frac{\tan u + \tan v}{1 - \tan u \tan v}. \tag{29}$$

Comparison of equations 28 and 29 leads us to choose:

$$\tan u = \tan \theta \quad \text{and} \quad \tan v = \left(\frac{Hf_\theta}{r^2 + Hrf_r}\right) \tag{30}$$

which yields equation 5.

## ACKNOWLEDGMENTS

*Portions of this work were supported by National Eye Institute (National Institutes of Health, Bethesda, MD) Grants EY-02994 to HCH and EY-08520 to RAA. RHR thanks Bertho Stultiens for helpful discussions.*

*The authors have no financial interest in the products described in the manuscript.*

*Received July 29, 1996; revision received April 22, 1997.*

## REFERENCES

1. Applegate RA, Howland HC. Noninvasive measurement of corneal topography. IEEE Eng Med Biol 1995;14:30–42.
2. Belin MW, Cambier JL, Nabors JR, Ratliff CD. PAR Corneal Topography System (PAR CTS): the clinical application of close-range photogrammetry. Optom Vis Sci 1995;72:828–37.
3. Applegate RA. Comments on Dr. Robert's article entitled: Characterization of the inherent error in a spherically-biased corneal topography system in mapping a radially aspheric surface. Refract Corneal Surg 1994;10:113–4.
4. Klein SA. Uniqueness of corneal shape from placido ring images. In: Vision Science and its Applications. vol 1. Technical Digest Series. Washington, DC: Optical Society of America 1996;204–7.
5. Klein SA. Corneal topography reconstruction algorithm that avoids the skew ray ambiguity and the skew ray error. Optom Vis Sci 1997; 74:945–62.

**Richard H. Rand**
*Department of Theoretical and Applied Mechanics*
*Cornell University*
*Ithaca, New York 14853*
*email: rand@rand.tam.cornell.edu*